EurJOC
European Journal of Organic Chemistry

A Journal of
ChemPubSoc Europe

Accepted Article

Title: Awkwardly-shaped dimers, capsules and tetramers: molecular and supramolecular motifs in C5-arylated chiral calixsalens

Authors: Małgorzata Petryk, Agnieszka Janiak, Leonard J. Barbour, and Marcin Kwit

To be cited as: *Eur. J. Org. Chem.* 10.1002/ejoc.201800314

Link to VoR: http://dx.doi.org/10.1002/ejoc.201800314

Supported by
ACES Asian Chemical Editorial Society

WILEY-VCH

10.1002/ejoc.201800314

WILEY-VCH

Awkwardly-shaped dimers, capsules and tetramers: molecular and supramolecular motifs in C5-arylated chiral calixsalens

Małgorzata Petryk,[a],[b] Agnieszka Janiak,*[a],[c] Leonard J. Barbour,[c] and Marcin Kwit*[a],[b]

Dedicated to Prof. Urszula Rychlewska on the occasion of her anniversary

Abstract: A series of novel C-5 arylated calixsalens synthesized *via* [3+3] cyclocondensation of *trans*-(*R*,*R*)-1,2-diaminocyclohexane with 2-hydroxyisophthalaldehyde derivatives are presented. The non-symmetrical aryl substituents of the 1-naphthyl type may act as switches opening (**ON** conformation) or closing (**OFF** conformation) the macrocycle cavity. This group of macrocycles, depending on the kind of aryl substituent, is characterized by a large variety of supramolecular architectures. While the substitution of the calixsalen skeleton by 2,5-dimethoxybenzene groups promotes the formation of head-to-head capsules, the presence of 3,5-dimethylbenzene group favors the tail-to-tail dimers. Introduction of 2-naphthyl substituents, in turn, results in the formation of a supermolecule consisting of four monomers that exists only in the solid state. Such arrangements of macrocycles generate a truncated tetrahedron shaped cavity never previously observed for this type of macrocyclic compounds.

Introduction

Since their initial discoveries by Ruzicka, chiral macrocyclic structures of various kinds have become common synthetic targets in supramolecular, materials and medicinal chemistry.[1-4] The presence of different functionalities that may form binding domains within chiral macrocycle skeletons, together with specific combinations of conformational flexibility and bias, makes macrocycles attractive as ligands, catalysts and highly selective receptors.[5-11] Enantiopure, symmetrical, polyimine and polyamine macrocycles of triangular, rectangular or rhombic shapes constitute a subclass of chiral macrocyclic compounds.[12,13] These compounds are versatile ligands in stereoselective synthesis and efficient enantio-discriminating agents.[14] Among methods developed so far for chiral polyimine macrocycle synthesis, those based on the concept of Dynamic Covalent Chemistry provide molecules that are thermodynamically favored over acyclic oligomer(s). Reversibility of the reaction is not a sufficient prerequisite for macrocycle formation. The structural predisposition of substrates to form higher-order constructs of various shapes is the most important, however.[15-17]

The products of [3+3] cyclocondensation between vicinal chiral diamines of the *trans*-1,2-diaminecyclohexane (DACH) type and 2-hydroxyisopthalaldehyde derivatives, dubbed *calixsalens*,[18] are particularly attractive.[19] Calixsalens and their reduced congeners, *calixsalans*, are prone to form multi-metal complexes with and without contraction of the macrocycle ring, and are used in asymmetric synthesis, as receptors, and as porous materials.[14,19,20]

The general structure of the calixsalen macrocycle may be split into two parts. The upper-rim of the macrocycle (head) contains all polar imine and OH groups (see Figure 1a), and the latter have a profound effect on the macrocycle structure. The intramolecular OH•••N=C hydrogen bond cascade involving phenolic hydrogen and nitrogen imine atoms strongly stabilize the s-*trans* conformation of the aromatic linker.[18b] The lower-rim (tail) contains substituents attached to the macrocycle skeleton. The type and size of the substituent on the lower-rim controls the ability of calixsalens to form supramolecules.

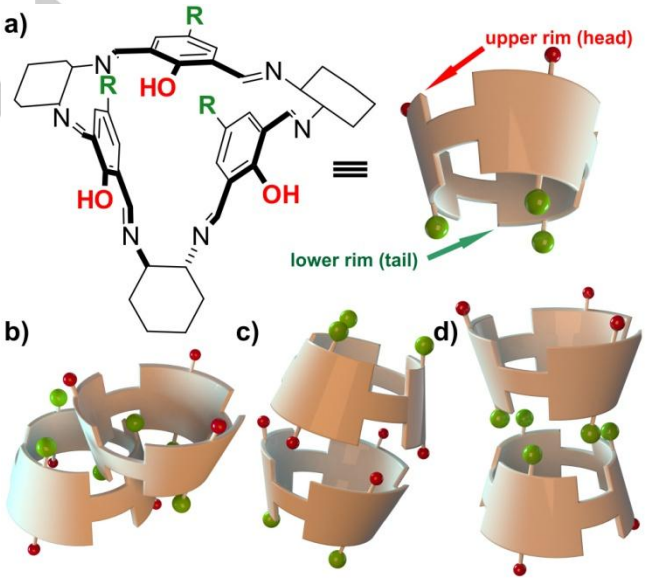

Figure 1. General structure of the calixsalen molecule a). Known types of host packing in calixsalen crystals: tail-to-tail dimer b) capsule c) and "a hourglass" d).

Macrocycles substituted at the C-5 position by small and/or polar groups such as halogens form mostly tail-to-tail dimers

[a] M. Petryk, Dr. A. Janiak, Dr. M. Kwit
Department of Chemistry, Adam Mickiewicz University
Umultowska 89B, 61 614 Poznan, Poland.
E-mail: agnieszk@amu.edu.pl, marcin.kwit@amu.edu.pl
[b] M. Petryk, Dr. M. Kwit
Center for Advanced Technologies, AMU
Umultowska 89C, 61 614 Poznan, Poland.
[c] Dr. A.Janiak, Prof. L. J. Barbour
Department of Chemistry and Polymer Science
University of Stellenbosch
7602, Stellenbosch, South Africa.

Supporting information for this article is given via a link at the end of the document.

(Figure 1b) by mutual insertion of one aromatic moiety of each monomer into the cavity of a partner. The formation of the tail-to-tail dimers is highly stereoselective and is driven solely by non-covalent interactions, such as dipole-dipole and π-π stacking.[21,22] Calixsalens having bulky groups of spherical symmetry at the C-5 position crystallize as capsules (head-to-head dimers) capable of solvent molecule entrapment (Figure 1c). The capsules are only stable in the solid state and decompose immediately after dissolution.[21]

C-5 Functionalization of the calixsalen skeleton by small OH groups increases hydrophilicity of the macrocycle lower rim and favors the formation of supramolecular organic frameworks, which consists of both the hourglass-like (Figure 1d) and capsule assemblies stabilized by hydrogen bonding networks. These coexist in the same crystal.[23]

The results reported so far clearly indicate that the possibilities for creating supramolecular systems from calixsalens are still unexplored. Thus, continuing our work on chiral functionalized macrocycles, we have extended our study to systems having aromatic units at the periphery of the calixsalen skeleton. The presence of a π-electron hydrophobic part may influence molecular conformation and solid-state supramolecular architecture of the given macrocycle. This in turn has helped to further our understanding of which structural factors control the processes of calixsalen assembly.

Taking the cyclocondensation as a turning point in synthesis, modification of the calixsalen structure is possible in two ways: either by modification of substrates (pre-cyclization approach) or by modification of the product (post-cyclization approach). However, the latter has limited applicability due to the instability of the imine bonds under harsh reaction conditions.

We decided to synthesize a series of 2-hydroxyisophthalic aldehydes, having various aryl substituents at the C-5 position[24] that were further used as substrates in cyclocondensation reactions with (*R*,*R*)-DACH. Representative calixsalens obtained in this way were further investigated by means of experimental and theoretical methods. Special emphasis was placed on single-crystal X-ray diffraction for the characterization of supramolecular assemblies in the solid state.

Results and Discussion

Synthesis

The general route to C-5 arylated calixsalens (**4a**-**4i**) is shown in Scheme 1. As the method of choice for synthesis of aldehydes **3a**-**3i** we employed palladium-catalyzed Suzuki reactions between 5-bromo-2-hydroxyisopthalaldehyde (**1**) and the respective boronic acids (**2a**-**2i**). In the majority of the cases, the isolated yields did not exceed 50% after column chromatography. The best result (64% yield) was obtained for the simplest 2-hydroxy-5-phenylisopthaldehyde (**2a**) (see Supplementary information, Table S1, entry 1). Either the boronic acids substituted by electron-withdrawing (**2d**) or electron-donating (**2g**) groups gave similar yields of the respective products, *ca* 50% (entries 4 and 7, Table S1 in the SI). Prolonging the reaction time and altering the conditions (change of catalyst, base and/or solvent) did not improve the results (all details regarding synthesis are given in the Experimental Section in the SI).

The macrocycles **4a**-**4i** were obtained by the reaction of equimolar amounts of the respective dialdehyde **3a**-**3i** and optically pure (1*R*,2*R*)-DACH, in dichloromethane solutions and under an inert atmosphere. The concentration of each substrate did not exceed 0.05 mol dm^{-3} and the reaction time was 24 hours. The products **4a**-**4i** were isolated and purified by dilution of the reaction mixture with methanol, filtration of the precipitate and crystallization from a dichloromethane-methanol or dichloromethane-acetonitrile mixture of solvents. This approach provided analytically pure **4a**-**4c** and **4g**-**4i** as yellow microcrystalline powders with yields ranging from 40 to 85% (see Table S1 in SI). The abovementioned procedure failed for calixsalens **4d**-**4f** and our attempts to purify the crude products either by precipitation or by crystallization were unsuccessful. For **4d**-**4f**, the yields of the trimeric products were estimated based on the ^{1}H NMR data only.

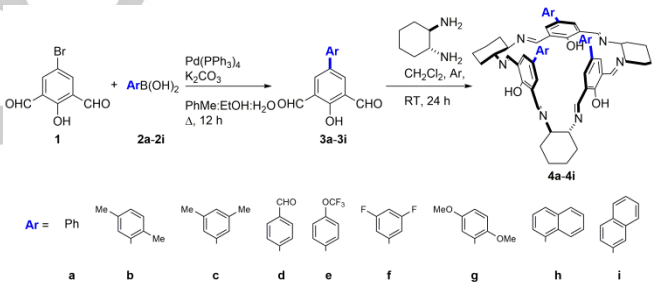

Scheme 1. The general procedure of synthesis of calixsalens **4a**-**4i** from C-5-aryl substituted aldehydes **3a**-**3i**.

The [3+3] trimeric structure of the pure **4a**-**4c** and **4g**-**4i** was confirmed by MS and HR MS analyses. The molecular ion peaks correspond to the $(M+H)^+$ ions of the [3+3] cyclocondensation products and no other products were detected. The ^{1}H NMR spectra of **4a**-**4c** and **4g**-**4i** measured in $CDCl_3$ showed the complete disappearance of aldehyde C<u>H</u>O signals, and two characteristic peaks for the imine C<u>H</u>N protons appeared at around 8.8 and 8.3±0.1 ppm (see Table S1 in SI), in agreement with the preferred s-*trans* conformation of the *bis*-imine system.[18b,21] The spectral regions between 8.1 and 6.5 ppm cover all C-H aromatic protons. These signals are slightly broadened at ambient temperature, apparently due to the hindered rotation around the aryl-aryl bond. The number of signals appearing in the aromatic region confirmed the C_3-symmetrical structure of the given macrocycle. Another characteristic feature found in the ^{1}H NMR spectra of the macrocycles under study is the position of O<u>H</u> signals, which appear at around 14.35±0.15 ppm (see Table S1 in SI), depending on the substituent at the C-5 position.

The reaction between DACH and aldehyde **3d** is a special case. We expected diverse reactivity of the formyl groups due to their different chemical surroundings. Two of the formyl groups are *ortho* with respect to the OH group; thus, one of the newly formed imine bonds will be stabilized by OH•••N hydrogen bonding. The third formyl group is the most accessible; however, there is no possibility for stabilization of the imine bond by hydrogen bonding. The cyclocondensation between equimolar amounts of (1*R*,2*R*)-DACH and **3d** provided a [3+3] macrocycle as the major product, as confirmed by MS analysis. The ^{1}H NMR spectrum of crude **4d** did not show the CHO signals from the formyl groups surrounding the OH group. The two peaks of the CH=N imine protons appeared at around 8.76 and 8.34 ppm, whereas CHO signal (δ = 9.98) of the formyl group attached to aryl substituent at C-5 remains unchanged. Unfortunately, at the same time, the ^{1}H NMR spectrum of crude **4d** shows the presence of small amounts of contaminants (see Supplementary Information) and our attempts to purify the product have been unsuccessful thus far.

ON-OFF conformation of 4h from ^{1}H NMR and ECD measurements and DFT calculations

While the conformation of the macrocycle core is essentially invariant, the aryl substituents at the periphery may adopt different orientations to minimize steric repulsion between hydrogen atoms and/or substituents in *ortho* positions. The representative example for discussion of molecular conformation of those compounds is calixsalen **4h**.

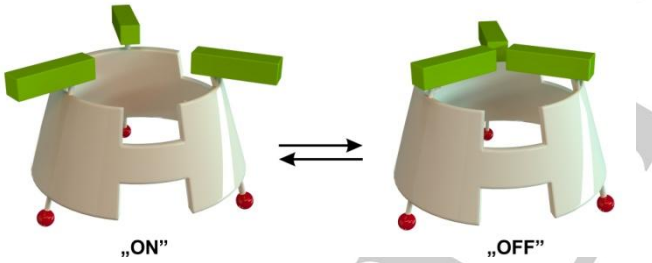

Scheme 2. **ON**-**OFF** conformational change in **4h**. The green boxes at the top of the vases represent non-symmetrical aryl substituents, red balls represent hydroxyl groups.

To shed light on the structural preference of calixsalen **4h** we performed in depth experimental and theoretical studies. Since X-ray diffraction data were unavailable for this particular case, the conformational dynamics of **4h** were determined primarily by comparison of experimental and calculated electronic circular dichroism (ECD) spectra and variable-temperature ^{1}H NMR measurements. It has been shown that agreement between experimental and calculated chiroptical properties unequivocally confirms not only the postulated favored structure of the given compound but also shed light on its conformational dynamics.[25]

For the non-symmetrical aryl substituents, such as 1-naphthyl, their relative orientations either opens the macrocycle cavity (**ON** state, open) or closes it (**OFF** state, closed), as presented in Scheme 2. The **ON** and **OFF** conformers represent the extreme cases characterized by C_3 symmetry and may exist in equilibrium with a number of conformers having C_1 symmetry, where one or two substituents is in either the closed or the open conformation.

The thermally-accessible structures of **4h** were obtained through a multi-steps computational procedure, involving (i) a systematic conformational search at the PM6 semi-empirical level;[26] (ii) geometry optimization of the first 100 low-energy conformers at the B3LYP/6-31G(d) level; (iii) re-optimization of the structures thus obtained at the B3LYP/6-311G(d,p) level employing the IEFPCM solvent model of chloroform;[27] (iv) calculations of the ECD spectra for the thermally-accessible structures, by employing CAM-B3LYP[28] and M06–2X[29] hybrid functionals, all in conjunction with the 6-311G(2d,2p) basis set and IEFPCM solvent model.[27] For each conformer the 150 electronic transitions were calculated. The calculated ECD spectra were Boltzmann averaged by taking into account conformers ranging from 0 to 2.0 kcal mol^{-1} in relative $\Delta\Delta G$ energies, following a generally accepted protocol.[25] The ECD spectra were simulated by overlapping Gaussian functions for each transition, with 0.4 eV at a half-height, according to the procedure previously described by Harada and Stephens.[30] Since the difference between ECD spectra calculated by means of both DFT methods were negligible, we only discuss the results obtained employing the CAM-B3LYP hybrid functional. The same protocol was applied to model compounds composed of one third of the parent macrocycle **4h** (the remaining results are deposited as supplementary material).

Temperature-dependent ^{1}H NMR spectra of **4h**, shown in Figure 2, confirm the preference of non-symmetrical over symmetrical conformers. At room temperature all signals in the diagnostic, aromatic region of the spectrum are averaged, which suggests rather unrestricted rotation of the aryl substituents. The most indicative CH=N peaks appear as a pair of singlets, which correspond to the s-*trans* conformation of *bis*-imine system and the overall C_3-symmetry of the molecule. Upon gradual cooling of the sample to -70 °C, broadening occurs at first, followed by signal splitting. The total number of CH=N signals increases to 14 and some of them are partially overlapped. A similar situation is observed for peaks originating from CH aromatic protons and from labile OH protons. The latter at the lower temperature are downfield shifted and split into five overlapped signals. The data obtained from ^{1}H NMR measurements suggest a rather complex conformational equilibrium rather than the existence a single conformer characterized by trivial C_1 symmetry.

This conclusion remains in agreement with theoretical results. As expected, calixsalen **4h** is not characterized by one low-energy structure in particular. The number of thermally accessible low-energy conformers reached 10. From them the $\Delta\Delta G$-based lowest energy conformer is also the most abundant (see Table 1 and Figures 3 and S1 in SI).

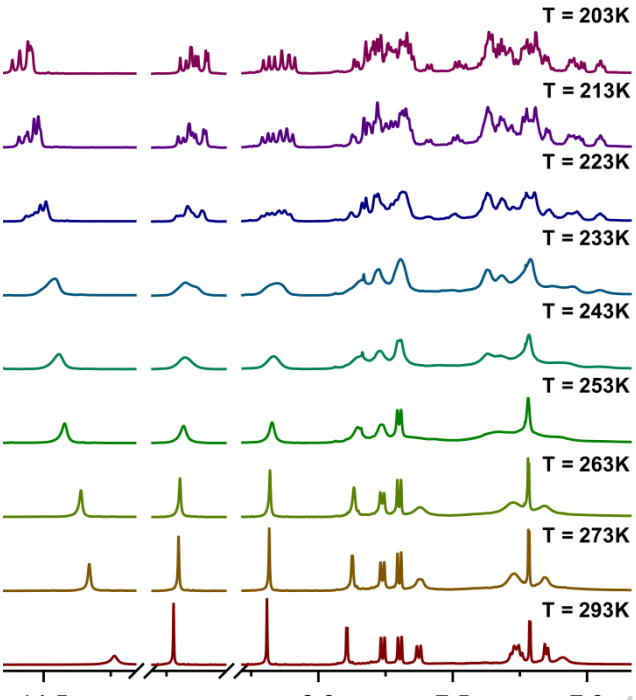

Figure 2. Traces of variable-temperature ^{1}H NMR spectra [CD_2Cl_2, 400 MHz] of calixsalen **4h**.

The characteristic feature of this and its related structures is the presence of O-H•••N intramolecular hydrogen bonds between hydroxyl groups and the imine nitrogen atoms in *syn* conformation that stabilize the macrocycle skeleton.[21] The conformation of the aryl substituent in each fragment of the molecule can be conveniently described in terms of *P* and *M* helicity, if we prioritize the imino group involved in hydrogen bonding over the non-hydrogen bonded one.[31] *P* Helicity is defined for 0° < *ω* < 180° and *M* is defined for twist angle *ω* adapting values between -180° and 0°, where *ω* is the angle defined by the sequence of C6-C5-C1'-C9' carbon atoms. The overall structure of the lowest energy conformer of **4h** is characterized by *P*,*P*,*M*-helicity of the biaryl moieties that correspond to *ω* values of 59, 124 and -120 degrees. It is more illustrative to describe this particular conformer as partially closed, since two of the three naphthyl groups are directed away from the centre of the macrocycle, whereas the third one closes the macrocycle cavity. This particular conformation is the superposition of a few opposing factors. First, conformers characterized by values of the *ω* angle equal to ±60° and ±120° represent the energetic minima. When one or more naphthyl groups adopt the closed conformation, the calculated dipole moment decreases. Additionally, the conformers having at least two groups closing the macrocycle cavity might be stabilized by CH•••π interactions between adjacent aromatic rings. However, the C_3-symmetrical **OFF** conformer is neither the energy minimum nor a stable structure, which is apparently due to the steric repulsions between the naphthalene groups. As a result, in the thermally accessible conformers of **4h** at least one of the naphthyl groups retains in open conformation.

At the final stage of the analysis we compared the experimental, the *ΔΔG*-based and the Boltzmann averaged calculated ECD spectra of **4h** (see Figure 3 and Figures S3-S6 in SI). It worth noting that the calculated ECD spectrum of **4h** is dominated by the most abundant the lowest-energy conformer no. 29 (see Figure S7 in SI).

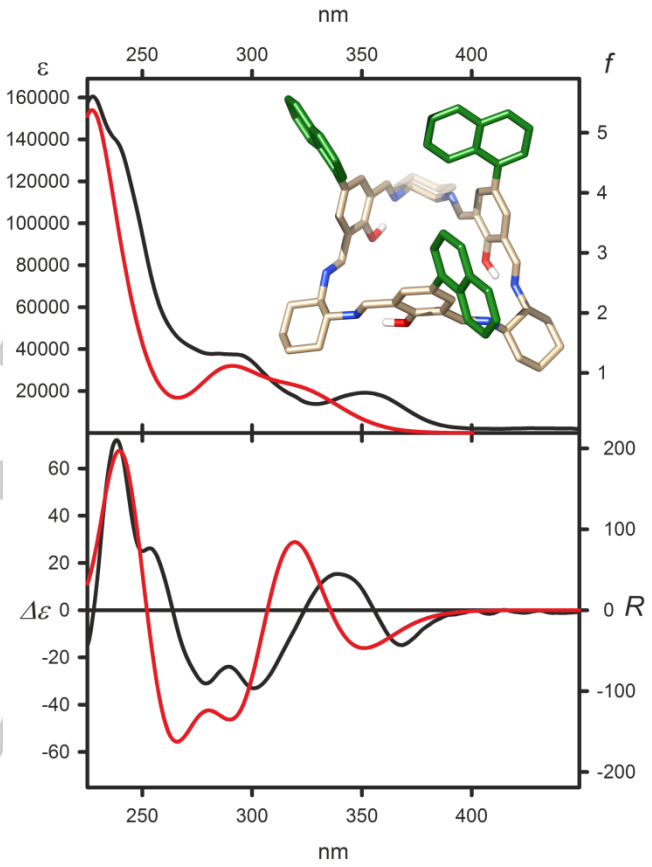

Figure 3. UV (upper panel) and ECD spectra (lower panel) of calixsalen **4h** measured in chloroform (black lines) and calculated at the IEFPCM/TD-CAM-B3LYP/6-311G(2d,2p) level and *ΔΔG*-based Boltzmann averaged (red lines). The calculated spectra were wavelength-corrected to match the experimental short-wavelength UV maximum. Insert shows structure of *ΔΔG*-based the lowest-energy conformer of **4h**, calculated at the IEFPCM/B3LYP/6-311G(d,p) level. For clarity some hydrogen atoms were omitted and naphthalene substituents were green-colored.

The experimental ECD spectrum of **4h** is rather complex and characterized by the presence of a negative exciton couplet corresponding to the UV absorption band around 350 nm, and by partially overlapping CD bands originating from the higher-energy electronic transitions. In the interpretation of the experimental ECD spectrum, calculations carried out for model compounds have become useful (see Supporting Information for details). In general, the ECD spectrum constitutes of two parts.

The lowest-energy exciton couplet and the negative Cotton effect at around 300 nm originate from electronic transitions within the macrocycle core (macrocycle **4h** without naphthalene subtituents). The low-energy electronic transitions involve imine chromophores. Since these transitions are polarized along the line connecting the nitrogen atoms, the negative sign of the low-energy exciton couplet is in agreement with the negative helicity of the N-C*-C*-N torsion angle (see Figure S8 in SI).

The higher-energy region of the ECD spectrum is dominated by the exciton interactions between the napthalene substituents. The negative exciton couplet originating from these interactions partially overlaps the Cotton effects from the macrocycle core. As a result, the higher energy region of the ECD spectrum displays the -/-/+ sequence of the Cotton effect. To summarize this paragraph, we may conclude that the calculated at the IEFPCM/CAM-B3LYP/6-311G(2d,2p) level and the Boltzmann averaged the ECD spectrum remains in very good agreement with the experimental one, by this way we confirmed the postulated preferred structure of the macrocycle **4h**.

Table 1. Relative energies (ΔE, $\Delta\Delta G$ in kcal mol^{-1}), percentage populations (Pop), values of ω angles (in degrees) and helicities calculated for individual conformers[a] of **4h** at the IEFPCM/B3LYP/6-311G(d,p) level of theory.

Conformer no	ΔE	Pop	$\Delta\Delta G$	Pop	ω			Helicity
4	0.28	12	1.10	7	-120	-122	61	*MMP*
29	0.60	7	0.00	43	-120	124	60	*MPP*
31	0.53	7	1.31	5	-127	-65	123	*MMP*
34	0.23	13	1.10	7	-59	123	126	*MPP*
50	0.00	18	1.62	3	-57	-60	125	*MMP*
69	0.39	9	0.71	13	-119	59	60	*MPP*
64	0.65	6	1.38	4	-58	-63	-128	*MMM*
89	0.38	10	1.02	8	-59	-62	57	*MMP*
94	0.47	8	1.05	7	-58	61	124	*MPP*
100	0.28	11	1.37	3	-64	59	123	*MPP*

[a] conformers are number according to their appearance in conformational search

Solid-state supramolecular architectures of 4c, 4g and 4i

Crystallization experiments were carried out using common organic solvents; however, it was not possible to obtain crystals in most cases. However, after many attempts, we were able to grow the crystals of **4c**, **4g** and **4i** by slow evaporation from acetone (**4i**), acetonitrile (**4g**) and a mixture of acetonitrile and dichloromethane (**4c**) solutions at room temperature. Calixsalens **4c**, **4g** and **4i** form inclusion crystals with the solvent used for crystallization. Since all of the crystals investigated were unstable under ambient conditions and easily lose solvent, even at low temperature, the quality of the X-ray data recorded was poor. Consequently, it was not possible to reliably determine all positions of solvent molecules for most of the crystals. Therefore, their unresolved electron densities were treated with SQUEEZE, as implemented in Platon.[32] All details regarding SQUEEZE treatment are provided in the SI.

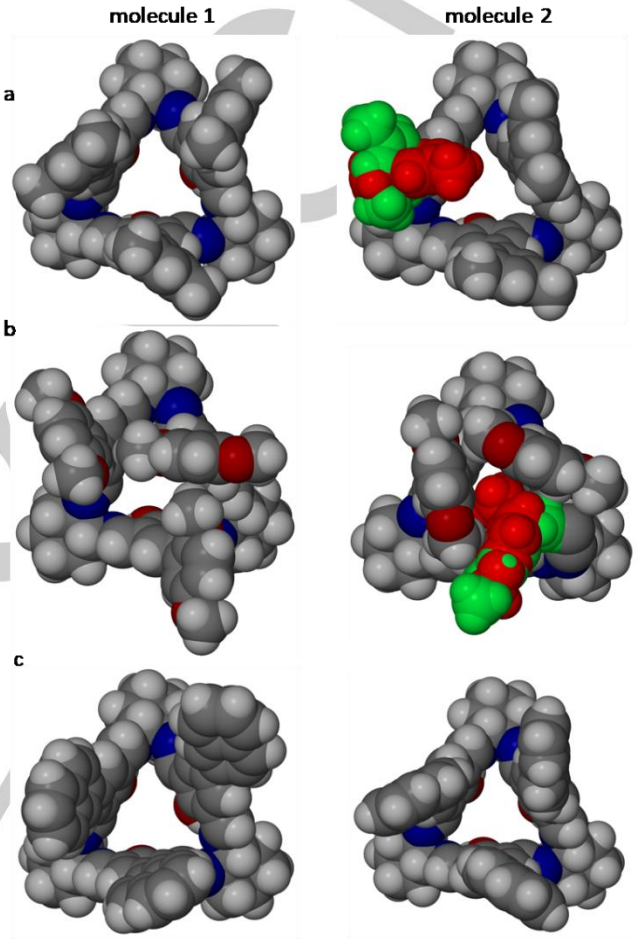

Figure 4. Orientation of the C-5 peripheral substituents in the symmetry-independent molecules of **4c** (a), **4g** (b) and **4i** (c). The disordered moieties of molecule 2 in crystals **4c** and **4g** are shown in red and green.

The single-crystal X-ray diffraction analyses revealed that C-5 arylated calixsalens **4c** and **4g** crystallize in the orthorhombic space group $P2_12_12_1$ while **4i** crystallizes in the trigonal space group $R32$. The asymmetric units of **4c** and **4g** each consist of two symmetry-independent macrocycles that occupy general positions. While one molecule in both structures is completely ordered, the other displays disorder that involves one of the three peripheral substituents. The disordered model considers that atoms of the C-5 aryl substituent can be split over two equivalent positions. Despite the fact that calixsalens **4c** and **4g** formally have C_3 symmetry, they remain unsymmetrical in the solid state. On the other hand, **4i**, crystallizes with one molecule in a general position and the other molecule situated on a three-

fold axis. Hence, its asymmetric unit contains one and a third molecules of **4i**. In structures **4c** and **4g** it was possible to locate some solvent molecules in the asymmetric unit. In both crystals the solvents occupy two different voids; while in **4c** one molecule of acetonitrille and half a DCM molecule are located in the extrinsic space. In **4g** two acetonitrille molecules occupy the intrinsic pores of the capsule.

The two symmetry-independent macrocycles in the structures of **4c**, **4g** and **4i** differ subtly in the orientation of the biaryl moieties and this effect may be enhanced in the presence of disorder. In **4c** the twist angle *ω* adopts values of -21, -38 and -53° in molecule 1, which corresponds to the *M*,*M*,*M* helicity of the biaryl moieties while in molecule 2, due to disorder, the helicity of the biaryl moieties can be described by sets of *ω* values that are either 54, -19 and -30° (*P*,*M*,*M*) for the **ON** state or -62, -19 and -30°(*M*,*M*,*M*) for the **OFF** state. In **4g**, the corresponding twist angle adopts values of 48, 51 and 81° in molecule 1, and 33, 40 and 61/54° in molecule 2. Thus, both macrocycles display the same *P*,*P*,*P*-helicity but different states (**ON**/**OFF**). While molecule 1 adopts a partially open conformation, in molecule 2 the peripheral substituents are directed towards the macrocyclic cavity and thus obscure its entrance. In turn, molecule 1 of **4i** is characterized by *P*,*P*,*P*-helicity that corresponds to *ω* values of 32, 33 and 37°, while molecule 2 displays the opposite *M*,*M*,*M*-helicity with all twist angle values of -38°. The van der Waals representations of the **4c**, **4g** and **4i** are shown in Figure 4.

In all crystals investigated, calixsalens display a diverse set of supramolecular architectures. In crystals of **4c** two symmetry-independent molecules self-assemble into a tail-to-tail dimer by mutual insertion of one of the biaryl moieties of each molecule into the cavity of the other macrocycle, as shown in Figure 5a. This dimeric arrangement, commonly observed in the crystals of calixsalen with small and/or polar groups at the C-5 positions, is stabilized by π•••π stacking interactions with short centroid-centroid distances of 3.645 Å and supported by numerous weak C-H•••π and C-H•••N interactions. Within the dimers, molecules are tilted toward each other by 70°.

Despite similarity in the size of the aryl substitutuents in **4c** and **4g**, these macrocycles self-assemble differently. Unlike **4c**, the two symmetry-independent molecules in **4g** are situated above each other in a head-to-head manner and are mutually twisted by about 60°. This arrangement promotes the formation of capsules (see Figure 5b). Each capsule thus obtained is stabilized by five C-H•••O intermolecular interactions (H•••O distances ranging from 2.34 to 2.68 Å). Symmetry expansion of the asymmetric unit shows that two neighboring capsules are mutually tilted by 74° and the intermolecular interactions between them are limited to the C-H•••π (mean H•••π distance is 2.83Å) and C-H•••O (H•••O distance is 2.64 Å) interactions. The solvent-accessible space of 212 $Å^3$ inside the capsule is fully occupied by acetonitrile molecules that can easily be removed from the cavity under ambient conditions. This tendency is supported by the open conformation of one of the two macrocycles constituting the capsules, which, in consequence, allows the solvent molecules to escape. Our previous studies show that this type of solid-state arrangement was observed in the crystals of chiral calixsalens substituted by bulky *tert*-butyl groups and in all racemic crystals having both large and small groups attached to the calixsalen skeleton.[21,22]

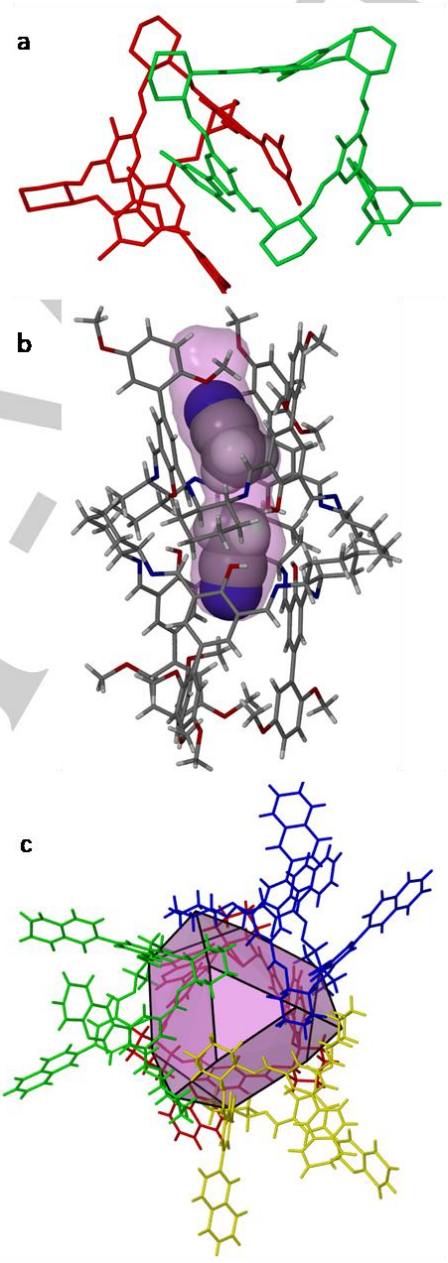

Figure 5. Perspective view of the supramolecular assemblies observed in the crystals investigated: a) The tail-to-tail dimer in **4c**, b) head-to-head capsule containing two solvent molecules in the void of 212 $Å^3$ in **4g** and tetramers with truncated tetrahedron shape voids volume of 732.864 $Å^3$ in **4i** c). The solvent accessible volume is shown as pink Connolly surfaces[33] using a probe radius of 1.5 Å. The guest molecules are shown as space-filling models.

In contrast, in the crystal structure of **4i**, two symmetry independent molecules display preferences to self-organize in a head-to-head manner. In this case, however, the arrangement

does not lead to dimers but rather favors the formation of large sized supermolecules that are constructed of three molecules of type 1 and one molecule of type 2 of **4i**. Such spherical arrangement of four neighboring macrocycles generate a truncated tetrahedron shaped cavity with a mean diameter of ca 8.5 Å and encloses 733 Å^3 of solvent occupied space, as shown in Figure 5c. Within the tetrameric capsule, the macrocyles are held together solely by weak C-H•••O and C-H•••π intermolecular interactions with H•••O distances of 2.65 Å and H•••π distances of 2.79 Å, respectively. Notably, this is the first observation of these types of head-to-head tetramers that are maintained by the weak non-covalent interactions and hence it represents an important extension to the known self-assembly of similar types of architecture that are mostly based on covalent bonds and/or hydrogen bonds. Extension of the crystal packing reveals interdigitation of the 2-naphthyl tails of the tetrameric supermolecules. Interestingly, this motif appears only between symmetry-independent macrocycles in which molecule 2 inserts one of the three 2-naphthyl substituents into the cavity of molecule 1 belonging to the neighboring supermolecule. In this assembly the intermolecular interaction is only observed between two 2-naphthyl moieties that are not parallel to each other; the dihedral angle between their planes is 52°. Such orientation of two moieties leads to formation of C-H•••π intermolecular interactions with H•••π distances of 2.78 Å that are responsible for stabilization of this supramolecular motif (see Figure 6).

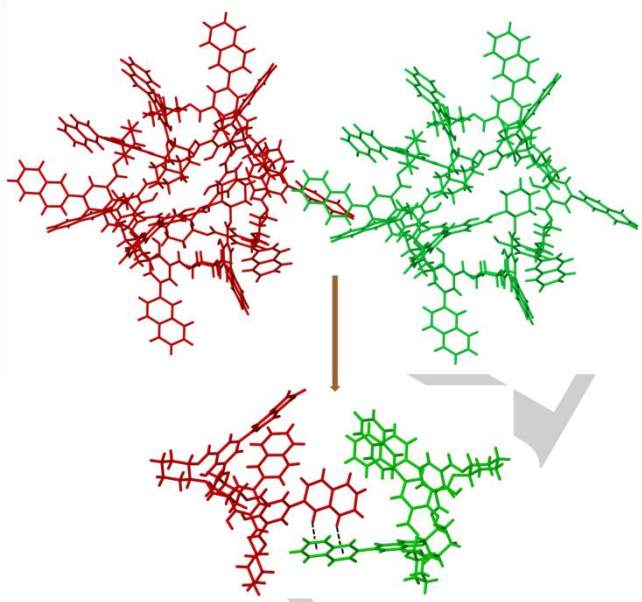

Figure 6. Packing mode of two neighboring supermolecules and their mutual interactions in the crystals of **4i**.

Conclusions

We have demonstrated the possibility for *egzo*-functionalization of calixsalen rings at the pre-cyclization stage through cycloimination between optically pure *trans*-1,2-diaminecyclohexane and the respective C-5 aryl substituted 2-hydroxyisopthaldehyde. The aldehydes are conveniently synthesized by Suzuki coupling.

Formal C_3 symmetry of the macrocycle (e.g. **4h**) is not evidenced in solution, as indicated by ECD spectra, variable-temperature ^{1}H NMR measurements and theoretical calculations. The same behavior is observed in the solid-state structures of **4c** and **4g**, but not in **4i**, which maintains formal C_3 symmetry in the crystals. Despite the presence of bulky substituents attached to the aromatic ring that potentially can prevent interdigitation in the solid state, this type of assembly is observed in crystals of **4c** and **4i**. However, in **4i** it does not lead to formation of the high-order structure in the solid state. Calixsalen **4i** forms supermolecules that consist of four monomers arranged in a head-to-head fashion and gives rise to a novel type of supramolecular architecture that has not previously been observed for this class of compounds.

Experimental Section

For synthetic procedures, full characterization of all new compounds, calculation details and X-ray diffraction experimental details see the Supporting Information. CCDC 1819412-1819414 contain the supplementary crystallographic data for this paper. These data can be obtained free of charge from The Cambridge Crystallographic Data Centre via www.ccdc.cam.ac.uk/data_request/cif.

Acknowledgements

The authors thank the National Science Centre in Poland, grants no UMO-2012/06/A/ST5/00230 (AJ, MK) and no 2017/24/T/ST5/00121 (MP), and the National Research Foundation of South Africa (AJ, LJB), for financial support. All calculations were performed at Poznan Supercomputing and Networking Centre (grant no 217).

Keywords: supramolecular assemblies • chiral calixsalens • tetrameric capsules • solid state architecture • egzo-functionalization

Conflict of interest

The authors declare no conflict of interest.

References

[1] E. Marsault, M. L. Peterson, *J. Med. Chem*. **2011**, *54*, 1961−2004.
[2] H. Höcker, *J. Chem. Chem. Eng*. **2009**, *58*, 73−80.
[3] A. T. Frank, N. S. Farina, N. Sawwan, O. R. Wauchope, M. Qi, E. M. Brzostowska, W. Chan, F. W. Grasso, P. Haberfield, A. Greer, *Mol. Diversity*, **2007**, *11*, 115−118.
[4] J. Xie, N. Bogliotti, *Chem. Rev*. **2014**, *114*, 7678−7739.

[5] T. Ogoshi, T. Yamagishi, Y. Nakamoto, *Chem. Rev*. **2016**, *116*, 7937−8002.
[6] X. Ma, Y. Zhao, *Chem. Rev*. **2015**, *115*, 7794−7839.
[7] H. Lu, N. Kobayashi, *Chem. Rev*. **2016**, *116*, 6184−6261.
[8] S. J. Barrow, S. Kasera, M. J. Rowland, J. del Barrio, O. A. Scherman, *Chem. Rev*. **2015**, *115*, 12320−12406.
[9] D. Zhang, A. Martinez, J.-P. Dutasta, *Chem. Rev*. **2017**, *117*, 4900−4942.
[10] D. M. Homden, C. Redshaw, *Chem. Rev*. **2008**, *108*, 5086–5130.
[11] N. Sakai, S. Matile, *Langmuir*, **2013**, *29*, 9031−9040.
[12] see for example: a) J. Gawronski, H. Kołbon, M. Kwit, A. Katrusiak, J. *Org. Chem*. **2000**, *65*, 5768-5773; b) M. Chadim, M. Buděsĭnský, J. Hodačová, J. Zavada, P. C. Junk, *Tetrahedron: Asym*, **2001**, *12*, 127-133; c) N. Kuhnert, A. M. Lopez-Periago, *Tetrahedron Lett*. **2002**, *43*, 3329-3332; d) N. Kuhnert, G. M. Rossignolo, A. M. Lopez-Periago, *Org. Biomol. Chem*. **2003**, *1*, 1157-1170; e) N. Kuhnert, A. M. Lopez-Periago, G. M. Rossignolo, *Org. Biomol. Chem*. **2005**, *3*, 524-537; f) N. Kuhnert, C. Straßnig , A. M. Lopez-Periago, *Tetrahedron: Asym*. **2002**, *13*, 123-128; g) N. Kuhnert, N. Burzlaff, C. Patel, A. Lopez-Periago, *Org. Biomol. Chem*. **2005**, *3*, 1911-1921; h) M. Kwit, P. Skowronek, H. Kołbon, J. Gawronski, *Chirality*, **2005**, *17*, S93-S100; i) J. Gawronski, M. Brzostowska, M. Kwit, A. Plutecka, U. Rychlewska, *J. Org. Chem*. **2005**, *70*, 10147-10150; j) Z. Wang, H. F. Nour, L. M. Roch, M. Guo, W. Li, K. K. Baldridge, A. C.−H. Sue, M. A. Olson, *J. Org. Chem*. **2017**, *82*, 2472−2480.
[13] M. Kwit, A. Plutecka, U. Rychlewska, J. Gawronski, A. F. Khlebnikov, S. I. Kozhushkov, K. Rauch, A. de Meijere, *Chem. Eur. J*. **2007**, *13*, 8688-8695.
[14] J. Gawronski, M. Kwit, U. Rychlewska in *Comprehensive Supramolecular Chemistry II*, *Vol. 3* (Ed.: J. L. Atwood), Elsevier, Oxford, **2017**, pp 267–291.
[15] a) N. E. Borisova, M. D. Reshetova, Y. A. Ustynyuk, *Chem. Rev*. **2007**, *107*, 46-79; b) S. Srimurugan, P. Suresh, B. Babu, H. N. Pati, *Mini Rev. Org. Chem*. **2008**, *5*, 228-242; c) V. Martí-Centelles, M. D. Pandey, M. I. Burguete, S. V. Luis, *Chem. Rev*. **2015**, *115*, 8736−8834.
[16] a) S. J. Rowan, S. J. Cantrill, G. R. L. Cousins, J. K. M. Sanders, J. F. Stoddart, *Angew. Chem. Int. Ed*. **2002**, *41*, 898−952; b) P. T. Corbett, J. Leclaire, L. Vial, K. R. West, J. L. Wietor, J. K. M. Sanders, S. Otto, *Chem. Rev*. **2006**, *106*, 3652−3711; c) Y. Jin, C. Yu, R. J. Denman, W. Zhang, *Chem. Soc. Rev*. **2013**, *42*, 6634−6654; d) S. P. Black, J. K. M. Sanders, A. R. Stefankiewicz, *Chem. Soc. Rev*. **2014**, *43*, 1861−1872.
[17] T. R. Cook, Y.-R. Zheng, P. J. Stang, *Chem. Rev*. **2013**, *113*, 734−777.
[18] a) S. R. Korupoju, P. S. Zacharias, *Chem. Commun*. **1998**, *12*, 1267-1268; b) M. Kwit, J. Gawronski, *Tetrahedron: Asym*, **2003**, *14*, 1303-1308.
[19] a) K. Tanaka, R. Shimoura, M. R. Caira, *Tetrahedron Lett*. **2010**, *51*, 449-452; b) K. Tanaka, T. Tsuchitani, N. Fukuda, A. Masumoto, R. Arakawa, *Tetrahedron: Asym*. **2012**, *23*, 205-208; c) Y. Fu, Z. Xing, C. Zhu, H. Yang, W. He, C. Zhu, Y. Cheng, *Tetrahedron Lett*. **2012**, *53*, 804-807; d) J. Gao, R. A. Zingaro, J. H. Reinspies, A. E. Martell, *Org. Lett*. **2004**, *6*, 2453-2455; e) J. Gao, J. H. Reibenspies, R. A. Zingaro, F. R. Woolley, A. E. Martell, A. Clearfield, *Inorg. Chem.* **2005**, *44*, 232-241; f) M. Paluch, J. Lisowski, T. Lis, *Dalton Trans*. **2006**, 381-388; g) M. Paluch, J. Lisowski, *J. Alloy. Compd.* **2008**, *451*, 443-447.
[20] J. Janczak, D. Prochowicz, J. Lewiński, D. Fairen-Jimenez, T. Bereta, J. Lisowski, *Chem. Eur. J*. **2016**, *22*, 598-609.
[21] a) M. Petryk, A. Troć, B. Gierczyk, W. Danikiewicz, M. Kwit, *Chem. Eur. J.* **2015**, *21*, 10318-10321; b) A. Janiak, M. Petryk, L. J. Barbour, M. Kwit, *Org. Biomol. Chem*. **2016**, *14*, 669-673.
[22] M. Petryk, K. Biniek, A. Janiak, M. Kwit, *CrystEngComm* **2016**, *18*, 4996-5003.
[23] M. Petryk, A. Janiak, M. Kwit, *CrystEngCom*, **2017**, *19*, 5825-5829.
[24] D. Reinhard, L. Schöttner, V. Brosius, F. Rominger, M. Mastalerz, *Eur. J. Org. Chem.* **2015**, 3274- 3285.
[25] M. Kwit, M. D. Rozwadowska, J. Gawronski, A. Grajewska, *J. Org. Chem*. **2009**, *74*, 8051–8063, and references cited therein.
[26] SCIGRESS 2.5, Fujitsu Ltd.
[27] M. J. Frisch et al, Gaussian 09, revision A.02, Gaussian, Inc., Wallingford CT, 2009.
[28] T. Yanai, D. Tew, N. Handy, *Chem. Phys. Lett.* **2004**, 393, 51-57.
[29] D. Jacquemin, E. A. Perpète, I. Ciofini, C. Adamo, R. Valero, Y. Zhao, D. G. Truhlar, *J. Chem. Theory Comput*. **2010**, *6*, 2071–2085.
[30] a) N. Harada, P. Stephens, *Chirality*, **2010**, *22*, 229-233; b) M. Kwit, J. Gawronski, D. R. Boyd, N. D. Sharma, M. Kaik, *Org. Biomol. Chem*. **2010**, *8*, 5635-5645.
[31] B. Testa, J. Caldwell, M. V Kisakürek, *Organic Stereochemistry, Guiding Principles and Biomedical Relevance*, Wiley-VCH, Weinheim, 2014.
[32] T. L. Spek, *Acta* Crystallogr. A, **1990**, *46,* 194-201.
[33] M. L. Connolly, *Science*, **1983**, *221*, 701-773.

10.1002/ejoc.201800314

WILEY-VCH

Entry for the Table of Contents (Please choose one layout)

Layout 1:

FULL PAPER

Novel *C-5*-functionalized calixsalens show substituent-driven self-association that can lead to the formation of supramolecules in the solid state.

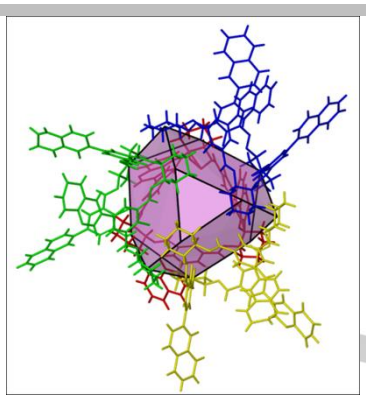

Key Topic*

Małgorzata Petryk, Agnieszka Janiak, Leonard J. Barbour, and Marcin Kwit **

Page No. – Page No.

Awkwardly-shaped dimers, capsules and tetramers: molecular and supramolecular motifs in C5-arylated chiral calixsalens

*calixsalen self-assembly